

Detection of Zn(II) ions by fluorescent pyrene-derived molecular probes

Erendra Manandhar^a, Peter J. Cragg^{b*} and Karl J. Wallace^{ab*}

^aDepartment of Chemistry and Biochemistry, Bobby Chain Technology Center (TEC), The University of Southern Mississippi, Rm 441A, 118 College Drive, Box #5043, Hattiesburg, MS 39406, USA; ^bSchool of Pharmacy and Biomolecular Sciences, University of Brighton, Brighton, UK

(Received 10 June 2013; accepted 12 August 2013)

Two pyrene-based molecular probes have been synthesised from *ortho*- and *meta*-bis(azidodimethyl)benzene and their coordination with Fe(III), Al(III), Fe(II), Zn(II), Ni(II), Cu(II), Cd(II), Hg(II), Ca(II), Mg(II) and Na(I) cations is described. The greatest spectral changes were observed with Zn(II) salts, which are important analytical targets in environmental and biological chemistry, and a detailed investigation on the influence of the counter-ion (F⁻, Cl⁻, Br⁻, I⁻, ClO₄⁻, NO₃⁻, CH₃CO₂⁻, SO₄²⁻ and BF₄⁻) was undertaken. Density functional theory studies suggest that Zn(II) is bound in the cleft of the probes in a 1:1 host:guest ratio. A significant hypsochromic shift is observed in the excimer band in the presence of metal salts and is greatest upon the addition of Zn(ClO₄)₂. The limit of Zn(II) detection is in the nanomolar range for the *meta*-isomer and the binding process is reversible allowing the system to be recycled several times. A protocol is proposed that would allow detection of Zn(II) in aqueous samples.

Keywords: zinc; pyrene; excimers; fluorescence sensors; DFT

Introduction

The development of molecular podands and tripodal molecular species to selectively bind guest species is an area of continued interest (1), especially where it relates to biologically and environmentally important analytes (2). Molecular receptors that change their spectroscopic signatures upon the addition of metal cations *via* changes in fluorescence are attractive analytical tools as fluorescence signals are easily perturbed by changes in the fluorophore's local environment (3). The detection of Zn(II) is of particular interest both *in vitro* and *in vivo* due to its biological importance (4).

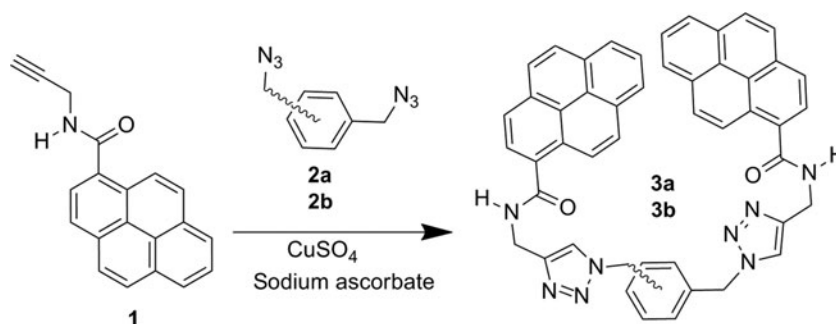
The human body contains ~2–3 g of zinc, mainly found within the confines of proteins and enzymes, which is essential to many biological functions (5); however, there is also a dark side to Zn(II). For example, it has been known since the mid-1980s that free zinc has an active role in neuronal injury (6) and there have since been numerous reports on the acute toxicity of free zinc and its link to neurodegenerative effects in Alzheimer's disease (4d, 7) and *amyotrophic lateral sclerosis* (Lou Gehrig's disease) (8). One of the major problems of Zn(II) ion detection is that it is spectroscopically silent and thus difficult to detect directly. Many fluorescence mechanisms have been used in molecular sensing and their applications in the field of supramolecular chemistry have been extensively reviewed (9). Numerous recent examples have incorporated the pyrene motif as a spectroscopic handle to detect ion pairs,

cations, anions and neutral species (2a). Many fluorescent Zn(II) sensors use an array of photophysical mechanisms, for example internal charge transfer (10), fluorescence resonance energy transfer (4k) or the heavy atom effect (11) and, more recently, chelation-enhanced fluorescence (CHEF) (12). The term CHEF was utilised in the early 1990s by Czarnik and co-workers (13) but has started to appear in the literature more frequently to describe a number of different mechanisms which include photo-induced electron transfer as well as manipulation of $n-\pi^*/\pi-\pi^*$ frontier orbitals. For a detailed discussion on these individual mechanisms, the reader is referred to de Silva's elegant review (9d).

We have recently reported the synthesis of a simple pyrene-based triazole receptor which was shown to self-assemble in the presence of ZnCl₂ by complexation-induced dimerisation (14). This was an example of a molecular dyad, whereby pyrene units are *syn* in orientation, and both cation and anion aided in the templation of the receptor. The fluorescent signal was generated by the self-assembled induced excimer formation upon the addition of Zn(II) ions.

The number of papers appearing on zinc sensors attests to the importance of this area of research and, consequently, the field warrants further development. Many groups have utilised different scaffolds, moieties and mechanisms to detect zinc in both aqueous (15) and non-aqueous systems (16). We now report a versatile

*Corresponding authors. Email: p.j.cragg@brighton.ac.uk; karl.wallace@usm.edu



Scheme 1. Synthesis of molecular receptors **3a** and **3b** (*ortho*-isomer (a) *meta*-isomer (b)).

modular approach to a pyrene-derived molecular probe in which two pyrene units are tethered to an aromatic backbone.

Results and discussion

The molecular probes contain an amide functional group and a triazole moiety attached to a benzene scaffold (*ortho*-derivative **3a** and *meta*-derivative **3b**). The functionalised pyrene group was prepared by reacting pyrene carboxylic acid with SOCl_2 to form the acid chloride, which was subsequently reacted with an equimolar amount of propargylamine and then purified by silica column chromatography to afford **1** in 60 % yield (17). Compound **1** was then reacted with bis(azidodimethyl)benzene (**2a** or **2b**) via an azide-alkyne Huisgen cycloaddition to afford the target molecule in $\sim 70\%$ yield (Scheme 1).

Fluorescence studies

Fluorescence analysis of compounds **3a** and **3b** with different metal ions Zn(II), Mg(II), Cd(II), Al(III), Hg(II), Ni(II), Cu(II), Fe(II), Fe(III) and Na(I) as either their chloride or perchlorate salts was initially tested with the addition of 10 equiv. of metal salts in CH_3CN , excited at 325 nm. There were no significant differences in the absorption spectra before or after the addition of metal ions and, therefore, no colorimetric tests were investigated in this study. The choice of either the chloride or perchlorate salt was due to their commercial availability and solubility in the chosen solvent system (Figure 1).

The fluorescence signal of the free receptors showed the typical monomer bands at 380 and 400 nm, characteristic of pyrene-derived compounds, which are assigned to the $\pi-\pi^*$ electron transitions (18). A very broad band at 495 nm is also seen which was assigned to

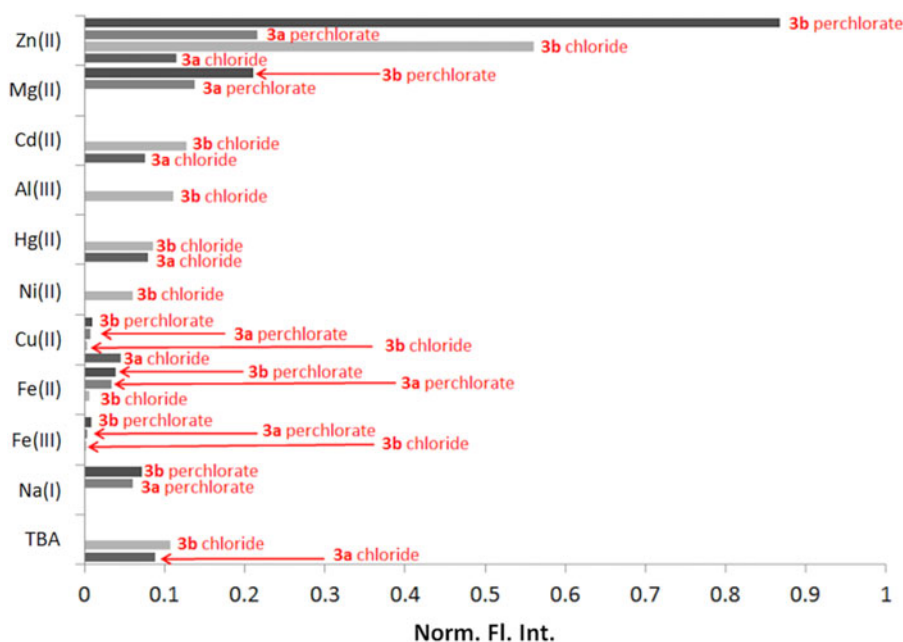


Figure 1. (Colour online) Fluorescence intensity of **3a** and **3b** upon addition of 10 equiv. of metal chlorides and perchlorates at 400 nm (CH_3CN , $\lambda_{\text{ex}} = 325$ nm).

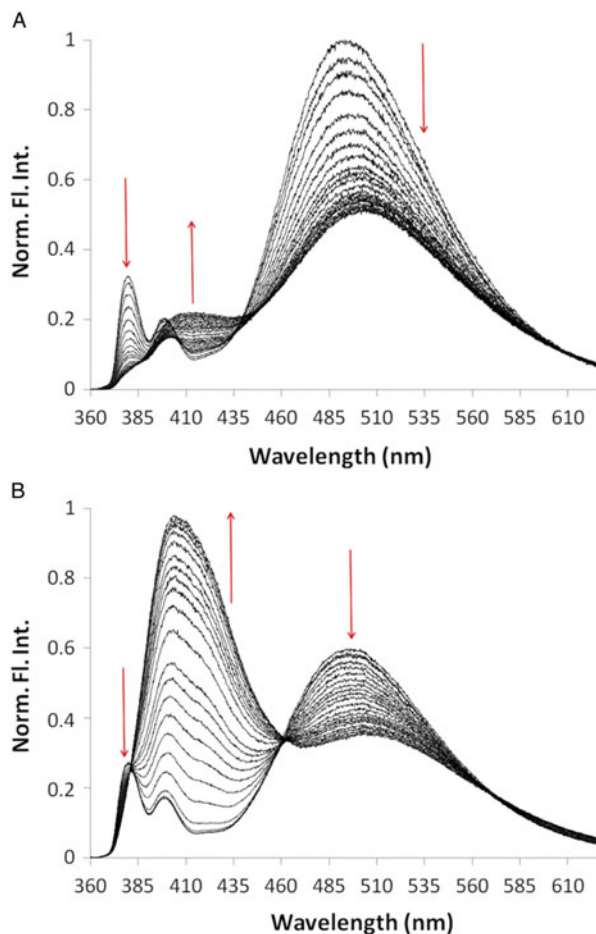


Figure 2. (Colour online) The fluorescence spectra of **3a** (A) and **3b** (B) upon incremental additions (up to 10 equiv.) of Zn(ClO₄)₂ (5 μM; CH₃CN, λ_{ex} = 325 nm).

intramolecular excimer formation, upon excitation at 325 nm. Intermolecular excimer formation was ruled out as the effect was observed in the micromolar range, whereas intermolecular excimer formation occurs at a concentration $> 1 \times 10^{-5}$ M. On inspection of the fluorescence spectrum, quenching was observed for all the metals except Zn(II) (and to a lesser degree Cd(II) and Mg(II)), and a new band was seen to increase at 400 nm. Upon addition of 10 equiv. of metal salts, it was evident that the Zn(II) salts showed significantly greater fluorescence at 400 nm for **3b** (Figure 2(B)) than for **3a**, for which a small increase in intensity was observed at 400 nm (Figure 2(A)).

The lack of fluorescence at 400 nm for **3a** is a consequence of the two pyrene units in **3a** adopting an *anti*-orientation which gives a greater pyrene–pyrene separation than is available to **3b**, in agreement with the density functional theory (DFT) calculations (*vide infra*) (see Figures S2–S4 for complete spectra).

There are many ways in which metals can quench fluorescence; transition metals such as Hg(II) enhance the

intersystem crossing from the excited state to the corresponding excited triplet state, known as the heavy atom effect, whereby the fluorescence is quenched by non-radiative decay. Redox active species such as Fe(III) and Cu(II) can quench the fluorescence by accepting an electron into their *d*-orbitals which was donated by the excited fluorophore (25). Therefore, it was not surprising that many of the metal salts studied quenched the fluorescence of our molecular probes. However, Zn(II) can neither accept an electron into its *d*-orbitals as they are already filled nor is it classified as a heavy metal. As a consequence, quenching is not observed and a signal ‘turn-on’ or fluorescence enhancement is seen.

It was clear, however, that the fluorescence intensity of the ClO₄[−] salt was more intense than that of the Cl[−] salt. We, therefore, explored the effect of different counter-ions on Zn(II) binding. The binding affinities of **3a** and **3b** towards Zn(II) salts (F[−], Cl[−], Br[−], I[−], NO₃[−], CH₃CO₂[−], SO₄^{2−}, BF₄[−] and ClO₄[−]) in CH₃CN were investigated using fluorescence spectroscopy at 298 K by excitation of a 5 μM solution of **3a** or **3b** at 325 nm (Figure 3).

There were significant spectroscopic changes upon the incremental addition of both Zn(ClO₄)₂ (Figure 2(A)) and Zn(BF₄)₂ (Figure 4). These large counter-ions seem to dissociate significantly in CH₃CN in comparison with the other anions studied. The excimer band at 495 nm shifted hypochromically with a new hyperchromic band appearing at 400 nm through an isoemissive point at 461 nm. Similar hypsochromic shifts have been observed by Nakahira et al. (19) and de Schryver et al. (20) in pyrene-based polymeric materials and bis(pyrenyl)ether derivatives, respectively. The binding affinities of **3a** and **3b** for Zn(ClO₄)₂, calculated using HypSpec (26), were $K_{11} = 1.4 \times 10^6$ and $3.8 \times 10^5 \text{ M}^{-1}$, respectively. The binding constants for all of the other zinc salts, including salts of Mg(II), Ca(II) and Na(I), are shown in Table 1. Interestingly, the binding affinity for Zn(ClO₄)₂ was a magnitude greater for **3a** than for **3b**, even though the

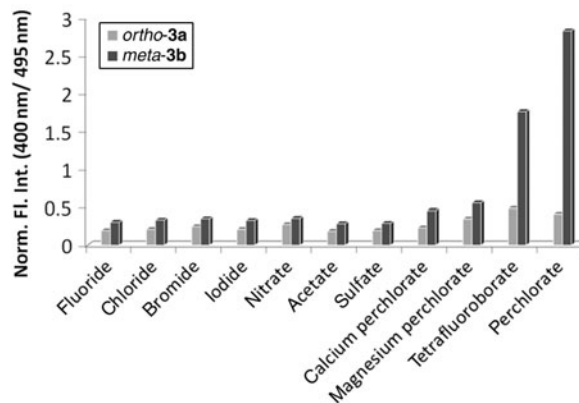


Figure 3. Fluorescence intensities of **3a** and **3b** with various Zn(II) salts.

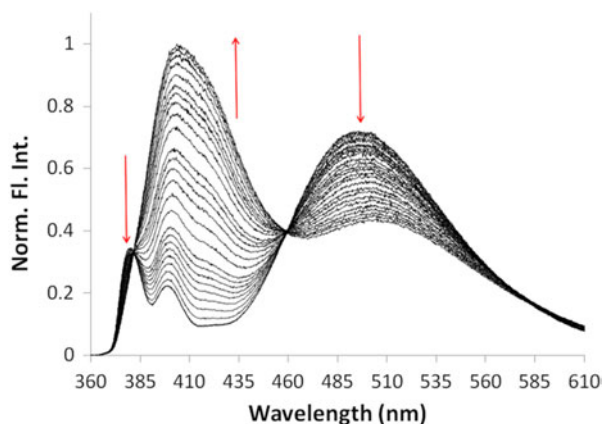


Figure 4. (Colour online) The fluorescence spectra of **3b** upon incremental 5 μM additions (up to 10 equiv.) of $\text{Zn}(\text{BF}_4)_2$ in CH_3CN ($\lambda_{\text{ex}} = 325 \text{ nm}$).

fluorescent change at 400 nm was not observed to be as dramatic (Figure 1).

In fact this trend is seen for all the other analytes studied, presumably due to the more favourable chelating motif. However, the lack of a spectroscopic signal can be justified due to the pyrene moieties adopting a *trans* orientation, in which they are further apart, thus reducing the magnitude of the electronic transition seen at 400 nm for receptor **3a**. These effects can be explained by the binding cleft of **3a** being more conducive to metal coordination than **3b** but its pyrene groups are further apart, reducing its fluorescence signal compared to **3b**.

We investigated the binding ability of **3b** systems in a mixed organic–water system, but only 1% water could be added to the system before precipitation occurred. Nevertheless, a similar ratiometric response is seen, with an excimer band decrease at 495 nm and increase at 400 nm, upon the addition of $\text{Zn}(\text{ClO}_4)_2$ (Figure S5). Poor aqueous solubility is often encountered for pyrene-based

Table 1. Association constants (K_{11}) between receptors **3a** and **3b** and ZnX_2 in CH_3CN . (a) could not be refined; however, based on the trend, the binding constant is predicted to be a magnitude larger than **3a**.

X	3a $K_{11} (\text{M}^{-1})$	3b $K_{11} (\text{M}^{-1})$
F^-	1.4×10^3	3.5×10^3
Cl^-	1.6×10^3	2.7×10^3
Br^-	1.1×10^4	1.2×10^4
I^-	9.6×10^3	5.4×10^4
NO_3^-	5.0×10^3	5.6×10^3
CH_3CO_2^-	1.8×10^3	9.9×10^2
SO_4^{2-}	3.1×10^4	5.7×10^3
BF_4^-	3.6×10^5	8.9×10^4
ClO_4^-	1.4×10^6	3.8×10^5
$\text{Mg}(\text{ClO}_4)_2$	9.1×10^3	a)
$\text{Ca}(\text{ClO}_4)_2$	8.4×10^2	5.3×10^2
$\text{Na}(\text{ClO}_4)$	4.5×10^2	1.7×10^2

metal probes and it is a major challenge to apply them to ‘real-world’ problems. Nevertheless, probes that can monitor zinc in non-aqueous systems such as CH_3CN (**16a**), THF (**16b**) and EtOH (**16c**) are often a good starting point from which an understanding of the binding properties of the molecular receptors may be gained. Recent work has taken this further and reports zinc binding either in mixed organic solvent–water or in 100% buffer solution (**15a**). To show that **3b** could, in principle, be used to assay $\text{Zn}(\text{II})$ found in aqueous samples, we developed a simple protocol. Solutions of **3b** in CH_3CN were refluxed with aqueous solutions of $\text{Zn}(\text{ClO}_4)_2$ between 0.0 and 0.5 mM for 24 h. The solvents were removed *in vacuo* and the residues were redissolved in CH_3CN . Fluorescence at 421 nm increased linearly with increasing $\text{Zn}(\text{II})$ concentration, demonstrating that receptor **3b** could be used to determine the zinc content of aqueous samples (Figures S6 and S7). We are currently preparing other molecular probes to improve solubility.

Molecular modelling and IR studies

Numerous efforts were made to grow crystals of the host–guest complex, to no avail. To gain insight into possible ligand and complex geometries, an extensive computational approach was adopted (**14**). Molecular mechanics calculations for **3a** and **3b** and their corresponding $\text{Zn}(\text{ClO}_4)_2$ complexes were carried out (Figure 5). Both the free receptors show interesting, but very different, π -stacked interactions. The *ortho*-isomer, **3a**, shows that the aromatic scaffold of the molecular probes participates in π -stacking and one of the pyrene arms seems to intercalate and form an intramolecular sandwich interaction (Figure 5(A)). This intercalation is not observed in the *meta*-isomer, **3b**, which shows 4.77 Å π – π distance between the two pyrene units. The distance was measured between the pyrene centroids (Figure 5(C)) and the C–H hydrogens on the triazole rings orientated towards the centre of the molecular probes. This is in excellent agreement with the interactions expected to generate the excimer band seen in the fluorescence spectrum. Both the $\text{Zn}(\text{II})$ complexes show drastically different optimised geometries. The $\text{Zn}(\text{II})$ ion is bound in a tetrahedral arrangement coordinated to the oxygen atom of the carbonyl functional group and a nitrogen atom in the triazole ring, forming a seven-membered chelating ring. The distance between two pyrene units in $[\text{Zn} \cdot \mathbf{3a}]^{2+}$ is 10.8 Å, whereas the distance between two pyrene units in $[\text{Zn} \cdot \mathbf{3b}]^{2+}$ is 5.5 Å, again in excellent agreement with the fluorescence data in which a broad excimer band is seen at 400 nm for the **3b** complex; the same band is significantly less intense for the **3a** complex.

In order to verify the binding mode of $\text{Zn}(\text{ClO}_4)_2$, suggested by the molecular modelling calculations, an IR study was conducted. The infrared spectrum of free

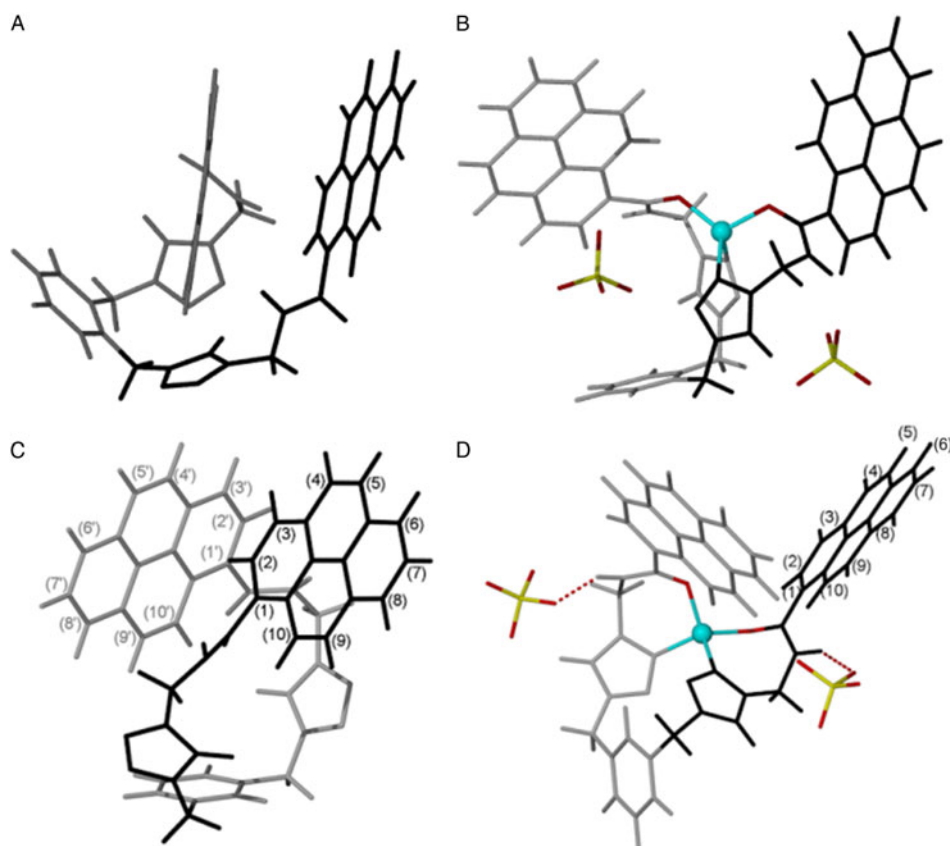


Figure 5. (Colour online) DFT fully optimised structures of (A) **3a**, (B) $[\text{Zn} \cdot \mathbf{3a}](\text{ClO}_4)_2$, (C) **3b** and (D) $[\text{Zn} \cdot \mathbf{3b}](\text{ClO}_4)_2$.

receptor **3b** was recorded as a solid using an ATR-IR and compared with that of the metal complex, prepared by grinding equimolar amounts of **3b** and $\text{Zn}(\text{ClO}_4)_2$ in a pestle and mortar for 30 min to form a green solid. This solid had been placed in the oven to dry for 2 h before the ATR-IR was recorded. Compound **3b** shows the characteristic IR bands for the amide functional group. The amide A stretch appears at 3333 cm^{-1} for the NH band. The amide I (C=O) stretch and the amide II (NH in plane bending) stretch are seen at 1639 and 1547 cm^{-1} in **3b**, respectively (Figure S8). It has been previously reported that significant infrared spectral changes occur when perchlorate coordinates to a metal ion through different modes (21). Determination of changing symmetry of the ClO_4^- ion upon binding, from T_d (ionic) to C_{3v} (unidentate) and C_{2v} (bidentate or bridging), can help identify the binding mode of the present system. The combination of the amide group in the molecular probe and the distinctively intense Cl–O stretching frequencies observed in the IR spectrum of the perchlorate anion makes these functional groups excellent IR handles to show that the proposed model is consistent with IR data. There is an increase in negative charge on the metal ion as the $\text{Zn} \cdots \text{O}$ bond becomes stronger, and both the amide I and amide II bands become weaker; this is

reflected in the IR wavelength shifts seen. Shifts of 46 and 16 cm^{-1} in the red direction for amide I and amide II, respectively, are seen. The amide A band is hypsochromically shifted by 48 cm^{-1} as a consequence of the hydrogen bonding interaction between the amide proton and one of the oxygen atoms in the ClO_4^- ion (Figure S8). The molecular models show that ClO_4^- participates in a number of hydrogen bonding interactions, lowering the symmetry of the ion from a T_d to a C_{3v} . As a consequence, the degeneracy of the T_2 (ν_3) Cl–O stretching absorption at 1059 cm^{-1} in the $\text{Zn}(\text{ClO}_4)_2$ salt is split into a doublet at 1070 and 1043 cm^{-1} assigned to A_1 (ν_1) plus E (ν_4) (22), which is in agreement with the binding present in the modelling calculations.

1D and 2D NMR studies

There is a significant overlap of the pyrene signals in the aromatic region of the ^1H NMR spectrum, rendering the exact assignment for receptor **3b** difficult. This is reasonable as there is free rotation around the methyl groups in the molecule, which makes the individual signals indistinguishable. Upon addition of 5 equiv. of $\text{Zn}(\text{ClO}_4)_2$, the aromatic pyrene protons shift to chemically different environments, presumably due to the conformational

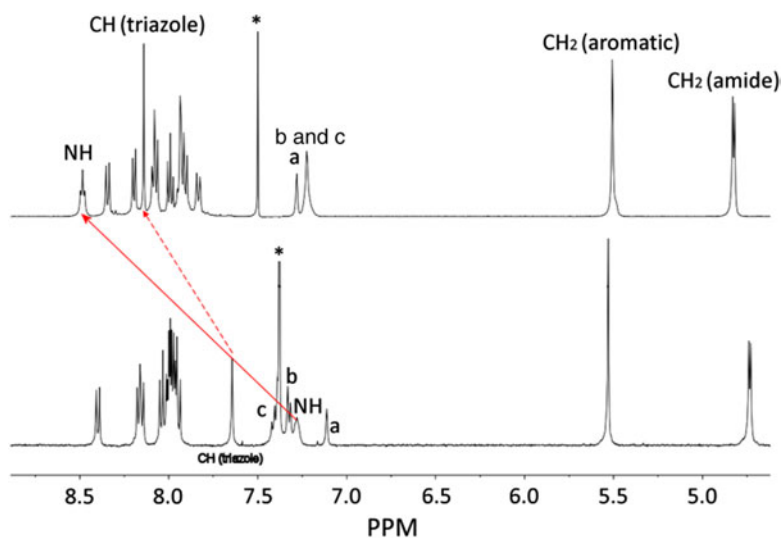


Figure 6. (Colour online) ^1H NMR complete spectrum (bottom) of receptor **3b** without the addition of $\text{Zn}(\text{ClO}_4)_2$ and (top) upon the addition of 5 equiv. of $\text{Zn}(\text{ClO}_4)_2$ in a mixture of $\text{CD}_3\text{Cl}:\text{CD}_3\text{CN}$ (1:1).

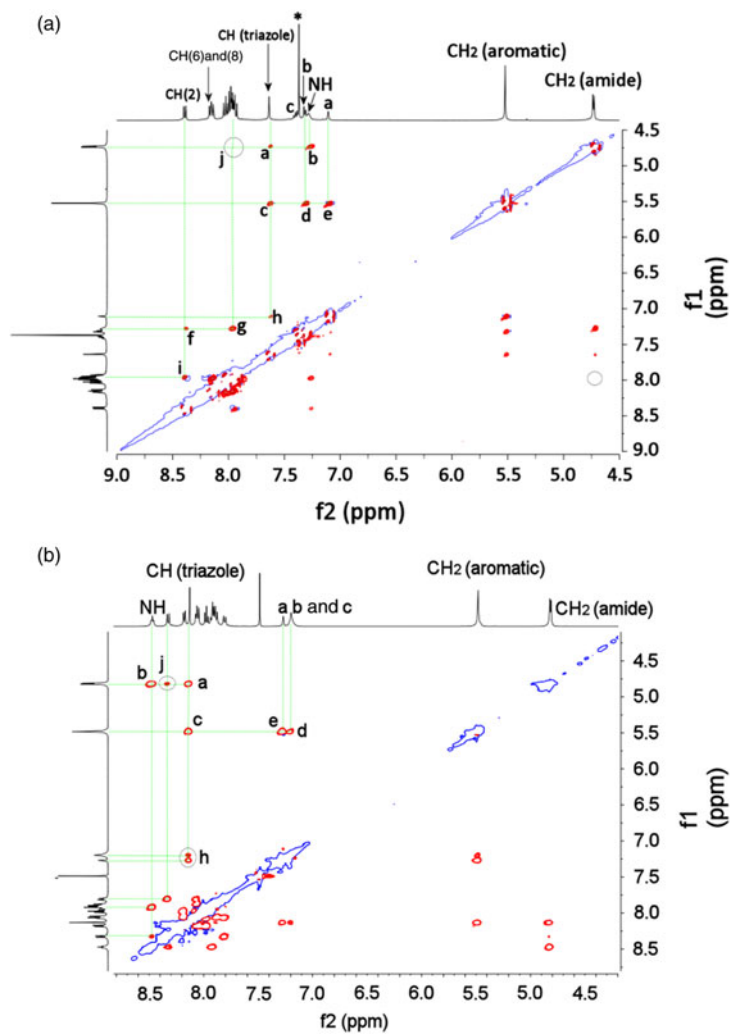


Figure 7. (Colour online) ROESY spectrum of **3b** (top) and after the addition of 5 equiv. of $\text{Zn}(\text{ClO}_4)_2$ (bottom) in a mixture of $\text{CD}_3\text{Cl}:\text{CD}_3\text{CN}$ (1:1).

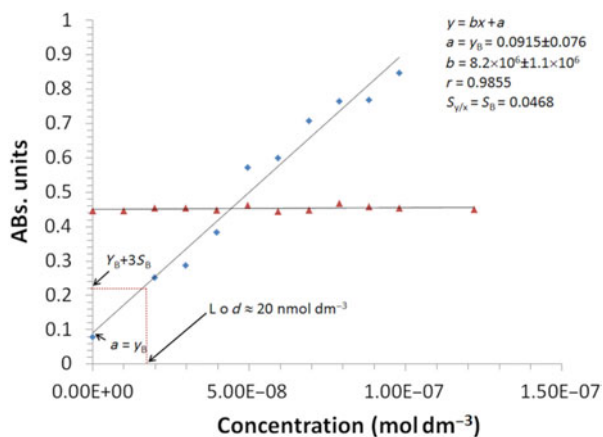


Figure 8. (Colour online) Calibration graph used to calculate the LoD for Zn(II) (blue diamonds) and Ca(II) (red triangles) with **3b** (20 nM; CH₃CN, $\lambda_{\text{ex}} = 325$ nm).

locking once Zn(II) ion has coordinated to the molecular cleft (Figure 6). The NH signal is shifted downfield by over 1 ppm due to increasing acidity of the NH proton upon coordination of the carbonyl oxygen atoms to the Zn(II) metal centre. This is in excellent agreement with our previously published work (14).

Upon addition of Zn(ClO₄)₂, distinct NMR chemical shifts were observed and careful 2D analysis (TOCSY, HSBC and HSQC, see Supporting Information – Figures S9–S21) allowed accurate assignments to be made. The 2D NMR spectroscopy, in particular ROESY, was helpful in the structural elucidation of the complex (Figure 7). The rOe spectrum recorded for **3b** in a mixture of CD₃CN and CDCl₃ (1:1, v/v) showed one very weak and nine strong rOe signals (Figure 7, top, see Supporting Information for full assignments).

Upon addition of zinc salt, two distinct signals became significant. The rOe between CH on the pyrene (C(2)

pyrene) and CH₂ adjacent to the NH functional group is absent in the free receptor ligand. Upon addition of Zn(ClO₄)₂, a strong distinctive rOe signal was seen between these same hydrogen atoms (labelled **j** in Figure 7, bottom). Presumably, upon addition of Zn(II) ion, the two oxygen atoms on the carbonyl coordinate to the metal centre causing a rotation of the amide group such that both the oxygen atoms participate in the coordination of Zn(II) within the cleft. This contrasts with the free receptor where the carbonyl functional groups point in opposite directions. This change in geometry is in agreement with the molecular modelling calculations.

Another two rOe signals of interest is between the triazole proton and *ortho*-proton of the benzyl group (Figure 7, bottom, labelled **h**). In the free receptor there is only one signal, whereas in the complex spectrum the triazole proton has two distinct rOe signals consistent with rotation of the benzyl functional group. Inspection of the molecular model (Figure 5) shows that the benzyl group is rotated by $\sim 70^\circ$. Unfortunately, the *ortho* (**3a**) isomer is insoluble at the concentration required for NMR and detailed 2D analysis was impossible.

Sensitivity and reversibility

At low concentrations (0.05 μM), **3b** showed an increase in the fluorescence intensity at 380 nm (the wavelength monitored in the detection studies at such low concentrations) upon the addition of Zn(ClO₄)₂. This is a key requirement for the molecular receptor if it is to be used to detect Zn(II) at biological concentrations: the same experiment with **3a** showed no spectroscopic change at the same concentration. To determine the limit of detection (LoD), the method of least squares was used to give a line of regression. The confidence limit of the slope is defined as $b \pm t_{\text{sb}}$, where t is the t -value taken from the desired confidence and $n - 2$ degrees of freedom. In our

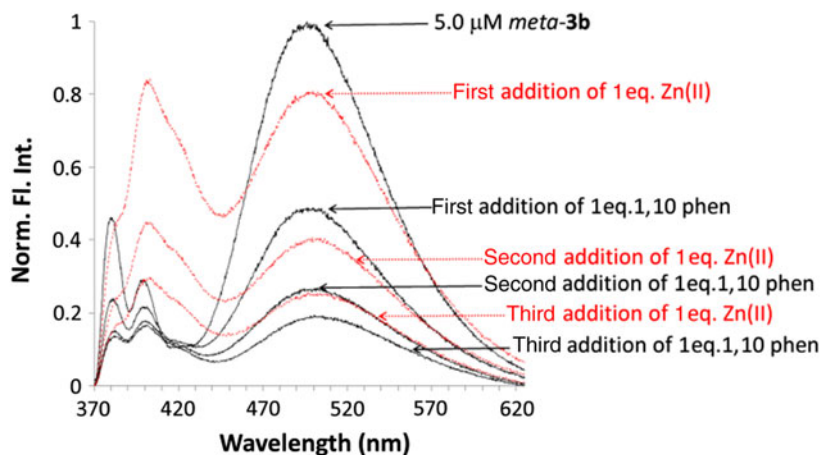


Figure 9. (Colour online) The effect of sequential addition of 1,10-phenanthroline and Zn(II) to **3b** (5.0 μM ; CH₃CN, $\lambda_{\text{ex}} = 325$ nm).

experiment, we chose a 95% confidence level (t -value 2.23, $df = 10$) (Figure 8). It is generally accepted that the LoD is the analyte concentration giving a signal equal to the blank signal plus three standard deviations from the blank, i.e. $y = y_B + 3S_B$. The calculated LoD values for **3a** and **3b** were 0.6 μM and 20 nM, respectively. Calcium salts often interfere with zinc in fluorescence assays; however, the Ca(II) complexes gave no spectroscopic responses in the same nanomolar concentration (Figure 8).

Upon addition of 1,10-phenanthroline, a known Zn(II) chelator, Zn(II), was 'stripped' from the molecular cleft. The fluorescence spectrum returned to that of the receptor although the intensity was $\sim 50\%$ of the original emission. This could be repeated three times (Figure 9), and each time 1,10-phenanthroline was removed, the intensity of the original emission was reduced by a further 50%. It is reasonable to assume that the quenching of fluorescence intensity is due to the 1,10-phenanthroline electron clouds being in proximity to the fluorophore of the molecular receptor, thereby preventing emission (25). This reversibility is essential if **3b** is to be incorporated into a Zn(II) sensor; we are currently investigating other chelators that strip Zn(II) without affecting the receptor fluorescence intensity.

Conclusions

In summary, two pyrene-based triazole molecular probes have been synthesised and shown to bind Zn(II) very effectively. Molecular modelling of $[\text{Zn} \cdot \mathbf{3a}]^{2+}$ and $[\text{Zn} \cdot \mathbf{3b}]^{2+}$ suggests that distances and angles between pyrene moieties in the two complexes are significantly different. This is consistent with fluorescence data that support excimer formation for $[\text{Zn} \cdot \mathbf{3b}]^{2+}$. Receptor **3b** has a LoD in the sub-nM range and its Zn(II) binding was shown to be reversible over several cycles. A protocol for use with aqueous samples has been developed and we are continuing our efforts to improve this method.

Experimental section

General

^1H , ^{13}C and 2D NMR spectra were recorded on a Bruker Ultrashield Plus 400 MHz spectrometer, Bruker Biospin Corporation, Billerica, MA, USA in the appropriate deuterated solvents. Chemical shifts are reported in parts per million (ppm) downfield from tetramethylsilane (0 ppm) as the internal standard and coupling constants (J) were recorded in Hertz (Hz). The multiplicities in the ^1H NMR spectra are reported as (br) broad, (s) singlet, (d) doublet, (dd) doublet of doublets, (ddd) doublet of doublet of doublets, (t) triplet, (sp) septet and (m) multiplet. All spectra were recorded at ambient temperature, unless stated otherwise, the abbreviations py(pyrene) and Ar(aromatic) are used to distinguish

between the two different aromatic proton signals. UV-vis experiments were carried out on a Beckman DU-70 spectrophotometer, Beckman Coulter, Inc., Brea, CA, USA. Low resolution mass spectra was measured on a Finnigan TSQ70 instrument Thermofisher Scientific, Waltham, MA, USA. IR spectra were recorded on a Nicolet Nexus 470 FT, Thermofisher Scientific, Waltham, MA, USA paired with a Smart Orbit ATR attachment. The characteristic functional groups are reported in wave numbers (cm^{-1}), and are described as weak (w), medium (m), strong (s) and very strong (vs). Fluorescence experiments were carried out on a QuantaMaster™ 40, Photon Technology International, Birmingham, NJ, USA intensity-based spectrofluorometer from PTI technologies in the steady state; slit widths 0.50 mm; $\lambda_{\text{ex}} = 325 \text{ nm}$, $\lambda_{\text{em}} = 360\text{--}625 \text{ nm}$. Elemental analysis was carried out at Atlantic Microlab, Inc., Atlanta, GA, USA. The synthesis and characterisation of compound **1** was previously reported (17).

Synthesis

General procedure for preparation of bis(azidomethyl)benzene

The desired (*ortho* or *meta*) bis(bromomethyl)benzene (1.32 g, 5.0 mmol) and sodium azide (0.97 g, 15 mmol) were dissolved in a 3:1 mixture of acetone and water (30 ml) and stirred at room temperature for 24 h (23). A mixture of dichloromethane (25 ml) and water (25 ml) was then added to the reaction mixture and stirred for 10 min. The organic layer was separated and washed three times with water (50 ml), dried over magnesium sulphate, filtered and the solvent was removed to produce a yellowish oil.

Characterisation of compound **2a**

Yield 752 mg, 4.0 mmol, 80%: ^1H NMR (300 K, DMSO, 400 MHz): δ 7.38 (m, 4H, CH_{Ar}), 4.45 (s, 4H, CH_2). ^{13}C NMR (300 K, DMSO, 100 MHz): δ 133.9, 130.0, 128.7, 51.0; IR (ATR solid); 2887 $\nu_{\text{C-H}}$ (w), 2085 $\nu_{\text{N}\equiv\text{N}}$ (vs) cm^{-1} .

Characterisation of **2b**

Yield 790 mg, 4.2 mmol, 84%: ^1H NMR (300 K, DMSO, 400 MHz): δ 7.38 (t, 1H, $J = 7 \text{ Hz}$, CH_{Ar}), 7.28–7.30 (m, 3H, CH_{Ar}), 4.37 (s, 4H, CH_2). ^{13}C NMR (300 K, DMSO, 100 MHz): δ 136.1, 129.2, 128.0, 53.4; IR (ATR solid); 2929 $\nu_{\text{C-H}}$ (w), 2086 $\nu_{\text{N}\equiv\text{N}}$ (vs) cm^{-1} .

General procedure for preparation of compounds **3a** and **3b**

N-(prop-2-ynyl)pyrene-1-carboxamide (17) (75 mg, 0.26 mmol) and the desired *ortho*- or *meta*-bis(azido-

methyl)benzene (25 mg, 0.13 mmol), copper(II) sulphate (3.25 mg, 0.013 mmol) and sodium ascorbate (5.15 mg, 0.026 mmol) were dissolved in a mixture of acetone and water (15 ml, 4:1) and stirred at room temperature for 48 h. The reaction mixture was then poured into ice-cold water (20 ml) to obtain a solid which was filtered, washed with water (200 ml) and dried to give the desired isomer.

Characterisation of compound **3a**

Yield 75 mg, 0.1 mmol, 77%; m.p. 244°C: $^1\text{H NMR}$ (300 K, DMSO- d_6 , 400 MHz): δ 9.24 (t, 2H, $J = 5$ Hz, NH), 8.47 (d, 2H, $J = 10$ Hz, CH_{py}), 8.35 (s, 1H, CH_{py}), 8.34 (s, 2H, CH_{py}), 8.32 (d, 2H, $J = 5$ Hz, CH_{py}), 8.29 (s, 1H, CH_{py}), 8.24 (d, 2H, $J = 10$ Hz, CH_{py}), 8.18–8.21 (m, 6H, CH_{py} and $\text{CH}_{\text{triazole}}$), 8.09–8.15 (m, 4H, CH_{py}), 7.37–7.39 (dd, 2H, $J = 3.5, 5.6$ Hz, CH_{Ar}), 7.20–7.22 (dd, 2H, $J = 3.5, 5.6$ Hz, CH_{Ar}), 5.89 (s, 4H, $\text{CH}_{2\text{triazole}}$), 4.69 (d, 4H, $J = 5$ Hz, $\text{CH}_2\text{N}_{\text{amide}}$). $^{13}\text{C NMR}$ (300 K, CDCl_3 , 100 MHz): δ 169.3, 134.8, 132.1, 131.9, 131.1, 130.6, 129.6, 129.3, 128.8, 128.7, 128.3, 127.6, 127.0, 126.3, 126.1, 125.7, 125.0, 124.8, 124.2, 124.1, 123.9, 50.4 and 35.5. ESI-MS m/z $[\text{M} + \text{H}]^+ = 755.4$ and $[\text{M} + \text{Na}]^+ = 777.5$; IR (ATR solid); 3339 ν_{NH} (m), 3115 ν_{CH} (w), 3037 ν_{CH} (w), 1633 ν_{CO} amide I (s), 1600 ν_{CO} amide II (m), cm^{-1} . Anal. Calcd for $\text{C}_{48}\text{H}_{34}\text{N}_8\text{O}_2$: H 4.54%; N 14.84%; C 76.38%; Anal. Recalcd for $\text{C}_{48}\text{H}_{34}\text{N}_8\text{O}_2 \cdot 9\text{H}_2\text{O} \cdot 10(\text{CH}_3)_2\text{CO}$: H 4.43%; N 14.32%; C 74.50%; found for $\text{C}_{48}\text{H}_{34}\text{N}_8\text{O}_2 \cdot 9\text{H}_2\text{O} \cdot 10(\text{CH}_3)_2\text{CO}$: H 4.72%; N 14.26%; C 74.47%.

Characterisation of compound **3b**

Yield 68 mg, 0.1 mmol, 69%; m.p. 195°C: $^1\text{H NMR}$ (300 K, DMSO, 400 MHz): δ 9.22 (t, 2H, $J = 5$ Hz, NH), 8.49 (d, 2H, $J = 10$ Hz, CH_{py}), 8.32–8.36 (m, 5H, CH_{py}), 8.30 (s, 1H, CH_{py}), 8.26 (s, 1H, CH_{py}), 8.20–8.24 (m, 7H, CH_{py} and $\text{CH}_{\text{triazole}}$), 8.09–8.13 (m, 4H, $\text{CH}_{\text{pyrene}}$), 7.40–7.43 (m, 2H, CH_{Ar}), 7.30–7.32 (d, 2H, $J = 8$ Hz, CH_{Ar}), 5.64 (s, 4H, $\text{CH}_{2\text{triazole}}$), 4.67 (d, 4H, $J = 5$ Hz, $\text{CH}_2\text{N}_{\text{amide}}$). $^{13}\text{C NMR}$ (300 K, CDCl_3 , 100 MHz): δ 169.3, 137.2, 132.1, 131.9, 131.2, 130.6, 129.7, 128.8, 128.6, 128.3, 128.2, 128.1, 127.6, 127.0, 126.3, 126.1, 125.7, 125.1, 124.8, 124.2, 124.1, 123.7, 53.0, 35.5. ESI-MS m/z $[\text{M} + \text{H}]^+ = 755.1$ and $[\text{M} + \text{Na}]^+ = 777.5$; IR (ATR solid); 3333 ν_{NH} (m), 3120 ν_{CH} (w), 3036 ν_{CH} (w), 1639 ν_{CO} amide I (s), 1547 ν_{CO} amide II (m), cm^{-1} . Anal. Calcd for $\text{C}_{48}\text{H}_{34}\text{N}_8\text{O}_2$: H 4.54%; N 14.84%; C 76.38%; Anal. Calcd for $\text{C}_{48}\text{H}_{34}\text{N}_8\text{O}_2 \cdot 10\text{H}_2\text{O} \cdot 35(\text{CH}_3)_2\text{CO}$: H 4.28%; N 14.01%; C 72.08%; found for $\text{C}_{48}\text{H}_{34}\text{N}_8\text{O}_2 \cdot 10\text{H}_2\text{O} \cdot 35(\text{CH}_3)_2\text{CO}$: H 4.91%; N 13.95%; C 71.87%.

UV-vis experiments

The general procedure for the molar absorptivity of compounds **3a** and **3b** was carried out as follows. A stock

solution (1.32×10^{-5} M) of compound **3a** was prepared by dissolving 0.5 mg in 50 ml of CH_3CN . Compound **3b** was prepared by dissolving 0.8 mg in 50 ml CH_3CN (2.12×10^{-5} M) and then 1 ml was transferred to the quartz cuvette. From the stock solution, eight successive dilutions were carried out, Table S1 shows the molar absorptivity calculated for each new compound.

Fluorescence experiments

A stock solution of compound **3** was prepared in CH_3CN . The solution was excited at $\lambda = 325$ nm and scanned from λ 360 to 625 nm with slit widths set to 0.5 mm. A 100 times more concentrated solution of the Zn(II) salt was prepared in CH_3CN and 10 μl (10 $\mu\text{l} = 0.5$ equiv. of metal salt) aliquots was added to compound **3**; fluorescence spectra were recorded after each addition. Dilution factors were taken into consideration upon binding study determination. The binding constants were determined from fluorescence titrations using HypSpec 2006 (26).

Computational methods

Equilibrium geometries for the ligands (**3a** and **3b**) and their zinc complexes ($[\text{Zn}\cdot\mathbf{3a}](\text{ClO}_4)_2$ and $[\text{Zn}\cdot\mathbf{3b}](\text{ClO}_4)_2$) were determined by full conformational searches of the 676 possible structures (identified through the number of rotatable bonds) followed by molecular mechanics energy minimisation methods (using the merck molecular force field). No formal bonds between zinc and ligands or anions were introduced. Initial refinement was followed by geometry optimisation at semi-empirical PM3d level with the resulting structures used as input coordinates for density functional calculations (B3LYP/6-31G*). Calculations were made using Spartan'10 installed on a desktop computer equipped with Intel Xenon Dual Quad Core CPUs running at 2.33 GHz (24).

Acknowledgements

KJW thanks the organisers of 2013 8-IMSIC (Profs Jeffery Davis, Amar Flood and Lyle Isaacs) held in Arlington for the invitation to write a manuscript for the special edition of *Supramolecular Chemistry* in honour of this event.

Funding

KJW thanks the NSF [OCE-0963064] for funding the ongoing research in the Wallace Laboratory.

Supplemental data

Supplemental data for this article can be accessed here: <http://dx.doi.org/10.1080/10610278.2013.835050>.

References

- (1) (a) Lee, M.H.; Kim, H.J.; Yoon, S.; Park, N.; Kim, J.S. *Org. Lett.* **2008**, *10*, 213–216; (b) Lee, M.H.; Wu, J.S.; Lee, J.W.; Jung, J.H.; Kim, J.S. *Org. Lett.* **2007**, *9*, 2501–2504; (c) Hossain, A.; Liljegren, J.A.; Powell, D.; Bowman-James, K. *Inorg. Chem.* **2004**, *43*, 3751–3755; (d) Petitjean, A.; Khoury, R.G.; Kyritsakas, N.; Lehn, J.M. *J. Am. Chem. Soc.* **2004**, *126*, 6637–6647; (e) Pintre, I.C.; Pierrefixe, S.; Hamilton, A.; Valderrey, V.; Bo, C.; Ballester, P. *Inorg. Chem.* **2012**, *51*, 4620–4635; (f) Do-Thanh, C.-L.; Rowland, M.M.; Best, M.D. *Tetrahedron* **2011**, *67*, 3803–3808; (g) Singh, N.; Kaur, N.; Callan, J.F. *J. Fluoresc.* **2009**, *19*, 649–654; (h) Wu, Z.-Q.; Li, C.-Z.; Feng, D.-J.; Jiang, X.-K.; Li, Z.-T. *Tetrahedron* **2006**, *62*, 11054–11062.
- (2) (a) Manandhar, E.; Wallace, K.J. *Inorg. Chim. Acta.* **2012**, *381*, 15–43; (b) McEwen, J.J.; Wallace, K.J. *Chem. Commun.* **2009**, 6339–6351; (c) Wallace, K.J. *Supramol. Chem.* **2008**, *21*, 89–102.
- (3) Barba-Bon, A.; Costero, A.M.; Gil, S.; Parra, M.; Soto, J.; Martínez-Máñez, R. *Chem. Commun.* **2012**, *48*, 3000–3002.
- (4) (a) Quin, W.-J.; Gee, K.R.; Kennedy, R.T. *Anal. Chem.* **2003**, *75*, 3468–3475; (b) Takeda, A. *BioMetals* **2001**, *14*, 343–351; (c) Sensi, S.L.; Paoletti, P.; Bush, A.I.; Sekler, I. *Nat. Rev. Neurosci.* **2009**, *10*, 780–791; (d) Frederickson, C.J.; Koh, J.-Y.; Bush, A.I. *Nat. Rev. Neurosci.* **2005**, *6*, 449–462; (e) Meeusen, J.W.; Nowakowski, A.; Petering, D.H. *Inorg. Chem.* **2012**, *51*, 3626–3632; (f) Jobe, K.; Brennan, C.H.; Motevalli, M.; Goldup, S.M.; Watkinson, M. *Chem. Commun.* **2011**, *47*, 6036–6038; (g) Tomat, E.; Lippard, S.J. *Inorg. Chem.* **2010**, *49*, 9113–9115; (h) Marnett, M.; Aragoni, M.C.; Arca, M.; Atzori, M.; Bencini, A.; Bazzicalupi, C.; Blake, A. J.; Caltagirone, C.; Devillanova, F.A.; Garau, A.; Hursthouse, M.B.; Isaia, F.; Lippolis, V.; Valtancoli, B. *Inorg. Chem.* **2009**, *48*, 9236–9249; (i) Aragay, G.; Alarcón, G.; Pons, J.; Font-Bardía, M.; Merkoçi, A. *J. Phys. Chem. C* **2012**, *116*, 1987–1994; (j) Michaels, H.A.; Murphy, C.S.; Clark, R.J.; Davidson, M.W.; Zhu, L. *Inorg. Chem.* **2010**, *49*, 4278–4287; (k) Sreenath, K.; Allen, J.R.; Davidson, M.W.; Zhu, L. *Chem. Commun.* **2011**, *47*, 11730–11732; (l) Kuang, G.-C.; Allen, J.R.; Baird, M.A.; Nguyen, B.T.; Zhang, L.; Morgan, T. J., Jr.; Levenson, C.W.; Davidson, M.W.; Zhu, L. *Inorg. Chem.* **2011**, *50*, 10493–10504; (m) Sain, D.A.; Babashkina, M.G.; Garcia, Y. *Dalton Trans.* **2013**, *42*, 1969–1972.
- (5) Frausto da Silva, J.J.R.; Williams, R.J.P. *The Inorganic Chemistry of Life*; 2nd ed. Oxford University Press: Oxford, 2001; pp. 315–340.
- (6) (a) Yokoyama, M.; Koh, J.-Y.; Choi, D.W. *Neurosci. Lett.* **1986**, *71*, 351–355; (b) Frederickson, C.J.; Hernandez, M. D.; McGinty, J.F. *Brain Res.* **1989**, *480*, 317–321.
- (7) Mathie, A.; Sutton, G.L.; Clarke, C.E.; Veale, E.L. *Pharmacol Ther* **2006**, *111*, 567–583.
- (8) Allen, M.J.; Lacroix, J.J.; Ramachandran, S.; Capone, R.; Whitlock, J.L.; Ghadge, G.D.; Arnsdorf, M.F.; Roos, R.P.; Lal, R. *Neurobiol. Dis.* **2012**, *45*, 831–838.
- (9) (a) Formica, M.; Fusi, V.; Giorgi, L.; Micheloni, M. *Coord. Chem. Rev.* **2012**, *256*, 170–192; (b) Drewry, J.A.; Gunning, P.T. *Coord. Chem. Rev.* **2011**, *255*, 459–472; (c) Valeur, B.; Leray, I. *Coord. Chem. Rev.* **2000**, *205*, 3–40; (d) de Silvia, A.P.; Nimal Gunaratne, H.Q.; Gunnlaugsson, T.; Huxley, A.J.M.; McCoy, C.P.; Rademacher, J.T.; Rice, T.E. *Chem. Rev.* **1997**, *97*, 1515–1566.
- (10) Hanaoka, K.; Muramatsu, Y.; Urano, Y.; Terai, T.; Nagano, T. *Chem. Eur. J.* **2010**, *16*, 568–752.
- (11) (a) Wang, H.-H.; Xue, L.; Fang, Z.-J.; Li, G.-P.; Jian, H. *New J. Chem.* **2010**, *34*, 1239–1242; (b) Kumar, M.; Kumar, M.; Bhalla, V. *Org. Lett.* **2011**, *13*, 366–369; (c) Smanmoo, S.; Nasomphan, W.; Tangboriboonrat, P. *Inorg. Chem. Commun.* **2011**, *14*, 351–354; (d) Varnes, A.W.; Dodson, R.B.; Wehry, E.L. *J. Am. Chem. Soc.* **1972**, *94*, 946–950.
- (12) El Majzoub, A.; Cadiou, C.; Dechamps-Olivier, I.; Tinant, B.; Chuburu, F. *Inorg. Chem.* **2011**, *50*, 4029–4038.
- (13) Akkaya, E.U.; Huston, M.E.; Czarnik, A.W. *J. Am. Chem. Soc.* **1990**, *112*, 3590–3593.
- (14) Manandhar, E.; Broome, J.H.; Myrick, J.; Lagrone, W.; Cragg, P.; Wallace, K.J. *Chem. Commun.* **2011**, *47*, 8796–8798.
- (15) (a) Zhou, X.; Yu, B.; Guo, Y.; Tang, X.; Zhang, H.; Liu, W.-J. *Inorg. Chem.* **2010**, *49*, 4002–4007; (b) Goswami, P.; Das, D. K. *J. Fluoresc.* **2012**, *22*, 1081–1085.
- (16) (a) Chen, H.; Wu, Y.; Cheng, Y.; Yang, H.; Li, F.; Yang, P.; Huang, C. *Inorg. Chem. Commun.* **2007**, *10*, 1413–1415; (b) Wu, Z.; Chen, Q.; Yang, G.; Xiao, C.; Liu, J.; Yang, S.; Ma, J.S. *Sens. Actuators B* **2004**, *99*, 511–515; (c) Zhou, X.; Li, P.; Shi, Z.; Tang, X.; Chen, C.; Liu, W. *Inorg. Chem.* **2012**, *51*, 9226–9231.
- (17) Hasegawa, T.; Umeda, M.; Numata, M.; Li, C.; Bae, A.-H.; Fujisawa, T.; Haraguchi, S.; Sakurai, K.; Shinkaia, S. *Carbohydr. Res.* **2006**, *341*, 35–40.
- (18) Birks, J.B. *Rep. Prog. Phys.* **1975**, *38*, 903–974.
- (19) Shoji, O.; Nakajima, D.; Annaka, M.; Yoshikuni, M.; Nakahira, T. *Polymer* **2002**, *43*, 1711–1714.
- (20) Collart, P.; Demeyer, K.; Toppet, S.; De Schryver, F.C. *Macromolecules* **1983**, *16*, 1391–1391.
- (21) Rosenthal, M.R. *J. Chem. Educ.* **1973**, *50*, 331–335.
- (22) (a) Herzberg, G. *Infrared and Raman Spectra*, Litton Educational Publishing, New York, **1944**; (b) Goldin, A.S.; Velten, R.J.; Frishkorn, G.W. *Anal. Chem.* **1959**, *31*, 1490–1492; (c) Armstrong, R.D.; Porter, D.F.; Thirsk, H.R. *J. Phys. Chem.* **1968**, *72*, 2300–2306.
- (23) Ramírez-López, P.; de la Torre, M.C.; Montenegro, H.E.; Asenjo, M.; Sierra, M.A. *Org. Lett.* **2008**, *10*, 3555–3558.
- (24) Spartan '10, Wavefunction, Inc., Irvine, CA, 2010.
- (25) Lakowicz, J.R. *Principles of Fluorescence Spectroscopy*; 3rd ed. Springer: New York, **2006**.
- (26) Gans, P.; Protonic Software, Leeds, **2006**.